Simulation-based Approach for Integrating Work within Heat Exchange Networks for Sub-ambient Processes

Homa Hamedi [a], Iftekhar A Karimi*[a] (cheiak@nus.edu.sg), Truls Gundersen[b] (truls.gundersen@ntnu.no)
[a]Department of Chemical and Biomolecular Engineering, National University of Singapore, 4 Engineering Drive 4, Singapore 117585.
[b]Department of Energy and Process Engineering, Norwegian University of Science and Technology, Kolbjorn Hejes v. 1A, NO-7491, Trondheim, Norway.

Abstract— Integrating work synergistically within heat exchange networks can offer considerable energy savings. Several publications have attempted to optimize this integration using a mathematical programming approach. However, the equation-based approach necessitates simplifications, and requires analytical correlations that often fail to reflect thermophysical properties accurately. In this article, the first simulation-based methodology is presented for work-integrated heat exchange network synthesis, which needs no correlations or simplifying assumptions. For this, a generalized superstructure is proposed, which not only accommodates the liquid and vapor-liquid phases, but also reduces the feasible search region for network synthesis. Particle swarm optimization has been used as the more suitable method for the proposed non-convex multi-modal simulation-based optimization problem. The methodology is illustrated using several scenarios of a literature case study on a liquid energy chain.

Keywords— work integration, heat integration, sub-ambient processes, meta-heuristic methods, particle swarm optimization, process optimization, process integration

1 Introduction

Enhancing the energy efficiency of an industrial facility is the first line of defense against the global concerns of energy, environmental pollution, carbon emissions, and climate change. Lowering specific energy consumption, while meeting product specifications, can help reduce fossil fuel use, GHG (Green House Gas) emissions, operating costs, and energy imports.

Heat exchange (HE) among process streams is by far the most studied form of energy integration that has had much impact in the chemical process industry (CPI), and has been applied to a number of processes (Li et al., 2019; Yang et al. 2019a). As shown in Figure 1, a heat exchange network (HEN) pairs the cooling and heating demands of process streams to

conserve thermal energy. It employs 2-stream exchangers along with utility heaters and coolers. However, work is also a major form of energy in the CPI, and it is natural to expound an analogous concept of work exchange (WE) as done by Huang and Fan (1996). As shown in Figure 1, a work exchange network (WEN) pairs the pressurization and depressurization needs of process streams to conserve mechanical energy. It uses work exchange devices (WEDs), pressure change units (PCUs), and motors/generators. While Huang and Fan (1996), Liu et al. (2014), and Amini-Rankouhi and Huang (2017) considered reciprocating pistons as WEDs for pairs of streams, Razib et al. (2012) considered single shafts hosting multiple streams. Razib et al. (2012) called them SSTCs (Single Shaft Compressor Turbine), where multiple PCUs (compression and turbine stages) and motors/generators may be mounted on a single shaft. Nair et al. (2018) compared and contrasted the concepts of HE and WE in detail.

In an attempt to address heat (temperature changes) and work (pressure changes) together, recent studies [Aspelund et al., 2007; Fu and Gundersen (2015a, 2015b, 2015c, 2015d, 2016a, 2016b)] have explored the concept of a work-integrated heat exchange network or WHEN (see Figure 1). The goal is to introduce pressure changes into an HEN via PCUs to (1) address the pressure needs of streams, and (2) enhance heat integration. Typically, minimizing exergy losses is the desired objective. However, this particular view or definition of a WHEN does not include WE, which was considered by Nair et al. (2018) in their work on WHENs. To recognize this nuance of WE between the two existing notions of a WHEN, we define HAWEN or Heat And Work Exchange Network (see Figure 1) that allows the exchanges of both work and heat. With that, Huang and Fan (1996), Razib et al. (2012), Liu et al. (2014), Amini-Rankouhi and Huang (2017), Zhuang et al. (2019) studied WENs, but Onishi et al. (2014b), Huang and Karimi (2016), and Nair et al. (2018) studied HAWENs. While this work focuses entirely on WHENs, the discussion here and Figure 1 present clarify the distinctions among WENs, WHENs, and HAWENs.

Figure 1 illustrates the physical features and units of various networks (HEN, WEN, WHEN, and HAWEN). To address their synthesis (WENS, HENS, WHENS, and HAWENS), two optimization approaches are common: pinch-based and superstructure-based. The pinch-based approach (Grossmann et al., 1998; Kamath et al., 2012; Quirante et al., 2018; Watson et al., 2015) uses the composite curves for HENS and identifies pinch points that limit the extent of heat integration. To integrate or introduce PCUs into an HEN, the pinch-based approach relies on the concept of exergy, and derives heuristics and guidelines that minimize exergy for specific scenarios. In contrast, the superstructure-based approach is simultaneous and more holistic. In place of CCs, pinch points, and exergy-based guidelines and heuristics, superstructures are constructed for potential integration options (Hasan et al., 2009a, 2009b; Huang and Karimi, 2016; Nair et al., 2018; Nair and Karimi, 2019; Onishi et al., 2014b; Yee et al., 1990; Yee and Grossmann 1990). Then, mathematical programming models are formulated that embed the relevant physical and thermodynamic constraints (e.g. temperature driving force for heat transfer). Given a suitable objective function, solving the resulting optimization problem gives the best integration network directly. The present work has used these two approaches in various combinations to address HENS, WENS, WHENS, and HAWENS. For instance, Aspelund et al. (2007) and Fu and Gundersen (2015a, 2015b, 2015c, 2015d, 2016a, 2016b) used the thermodynamic insight to propose several pinch-based guidelines and heuristics for WHENS. Onishi et al. (2014a) used the superstructure-based HENS in their WHENS work. Subsequently, Onishi et al. (2018) used a superstructure-based approach for WHENS but the pinch-based approach for HENS by Quirante et al. (2018). Razib et al. (2012) proposed a superstructure for WENS with SSTCs. Nair and Karimi (2019) proposed a novel stageless superstructure for HENS. Huang and Karimi (2016), Nair et al. (2018), and Onishi et al. (2014b) used superstructures for WENS and HENS in their models for HAWENS. An MINLP model is developed by Yu et al. (2019) using the Duran–Grossmann (1986) to identify

the optimal thermodynamic path of process streams. Pavão et al. (2019) proposed a model for WHENS using a stage-wise HEN. Then, a metaheuristic optimization framework (Simulated Annealing and Rocket Fireworks) was employed to solve the problem.

For HAWENS, Huang and Karimi (2016) and Onishi et al. (2014b) classified process streams into High vs. Low Pressure (HP vs. LP) and Hot vs. Cold (HS vs. CS). Onishi et al. (2014b) assumed that the HP streams cannot have end coolers, and LP streams cannot have end heaters. On the other hand, Huang and Karimi (2016) assumed no cooling before expansion and no heating before compression to minimize power consumption. Both these assumptions may remove some promising HAWEN solutions. In addition, both works made simplifying assumptions such as gaseous streams and constant thermophysical properties (e.g. zone-specific heat capacity, Joule-Thomson coefficient, and specific heat ratio). Later, Nair et al. (2018) removed the stream classifications and relaxed many of these assumptions, while using more or less a similar HAWENS superstructure (Figure 2). Their model does not label streams as LP/HP or hot/cold, allows liquid and 2-phase streams, and does not assume constant thermophysical parameters. However, their mathematical programming model necessitates an analytical or equation-based (vs. numerical or code-based) formulation. For example, thermophysical properties such as specific enthalpy and bubble/dew point temperatures must be expressed as explicit nonlinear correlations or functions of pressure, temperature, and composition, which must be developed using rigorous process simulators such as Aspen Plus, Aspen HYSYS and Unisim. Such correlations are typically easier for known stream compositions, which may be unknown in a process synthesis problem. Furthermore, representing the entire vapor-liquid phase diagram accurately may not be possible. This is quite crucial for sub-ambient processes in which even a small error in temperature may result in an infeasible solution.

To appreciate the importance of accurate properties, consider the results of case studies in Nair et al. (2018). They used SRK as the fluid package in Aspen HYSYS to derive their property correlations (Nair and Karimi, 2019). We simulated a few units of their networks in Aspen HYSYS using SRK. In Figure 3, the results in black are from their analytical correlations, and those in red are from Aspen HYSYS. For H-104 in Figure 3, for inlet temperatures of 197.3 K and 103.4 K and one outlet temperature of 190.4 K, we get the other outlet temperature as 144.8 K from Aspen HYSYS versus 135.5 K from their correlations. This is a significant mismatch. Similar analyses of other units such as valves and expanders also show significant departures (Figure 3) of their correlation-based predictions from Aspen HYSYS simulations. Such departures may misguide network optimization to suboptimal or even infeasible solutions. In other words, thermophysical properties from a process simulator should be preferred over analytical correlations.

While Nair et al. (2018) allowed liquid and 2-phase states in their HAWENS model, they did not include pumps and hydraulic expanders as PCUs in their superstructure. They also permitted a pressure ratio of one for a stream in a PCU and used that to model the stream bypassing that PCU. However, when this happens, the stream exits and reenters the HEN with no change (no PCU) in its conditions. This introduces redundant streams into the HEN. This not only increases the problem size of HENS, but also the combinatorial complexity, because the redundant streams can now again act as hot or cold streams. All these issues make their Mixed Integer Nonlinear Programming (MINLP) model less efficient computationally. Furthermore, Nair et al. (2018) did not remove several permutations in their superstructure. For instance, if a stream s needs only one stage of pressure change, then their superstructure allows K_s different options for this, where K_s is the maximum allowable PCU stages in Figure 2. Hence, we need a better and still tighter superstructure to enhance computational efficiency.

In summary, the existing WHEN superstructures suffer from some configurational limitations and computational inefficiencies. In this work, we present a more comprehensive and tighter superstructure for WHENS by eliminating permutations of stages and the aforementioned redundancies. We then propose a simulation-based optimization methodology for WHENS to exploit commercial process simulators to obtain thermophysical properties. Based on the previous literature (Cao et al. 2017; Hamedi et al., 2018; Hamedi et al., 2019; Sadeghzadeh et al., 2015), particle swarm optimization (PSO) offered a good option. Being a derivative-free methodology, PSO allowed us to make all the discrete synthesis decisions in terms of continuous variables, which reduced the number of optimization variables drastically. Finally, we illustrate the effectiveness of our approach on a case study on a liquefied energy chain (Aspelund et al., 2007, 2009a, 2009b) and present superior results.

2 Problem Statement

A sub-ambient process (e.g. cryogenic, refrigeration, liquefaction) has S streams ($s = 1 \dots S$) that include process streams and all utilities. All stream compositions are known and fixed throughout the process. The process stream flows are known, but utility stream flows are unknown. A utility may be used multiple times (separate streams) with different flow rates in the process. Each stream s enters the process at known inlet (initial) specific enthalpy HIN_s and pressure PIN_s. It must leave the process at known outlet (target) enthalpy $HOUT_s$ and pressure $POUT_s$. In this work, we aim to synthesize a process network (WHEN) that integrates the stated heat and work needs of the S streams at minimum total annualized cost (TAC) or minimum exergy consumption. The WHEN may use one multi-stream heat exchanger (MSHE), no 2-stream exchangers, and one or more stand-alone single-stream valves, pumps, turbines, hydraulic expanders, and compressors. We assume:

1. The line and MSHE pressure drops are zero for all streams in the entire WHEN.

2. Minimum temperature approach (MTA) in the MSHE must exceed a known lower limit (which can be close to zero also).

3. Each PCU (pump, valve, compressor, or turbine) is adiabatic.

3 Generalized Superstructure

Figure 4 presents our generalized superstructure for WHEN. It has $(S + 1)$ components: one superstructure for each stream s and one MSHE. While the overall architecture of our proposed superstructure is similar to those of Onishi et al. (2014a), Huang and Karimi (2016) and Nair et al. (2018), there are key differences as discussed later. In this work, the MSHE substitutes the single HEN that these works use.

As seen in Figure 4, the superstructure for a stream s consists of (K_s) stages, where K_s is assumed a priori. Each stream s must pass through stage 1, but it can bypass any other stage. While Stage 1 comprises only the single shared HEN, Stages 2 through K_s have two substages each. The first substage is Pressure Changing Stage (PCS) denoted by (PCS_{sk}) for stream s and stage k, and the second substage is the one shared HEN. As shown in Figure 5, each PCS_{sk} has a 2-phase separator followed by two parallel PCU trains. One PCU train is for the liquid substream from the separator, and the other for the gas substream. The gas train has a compressor, turbine, and valve as potential PCUs, while the liquid train has a pump, hydraulic expander, and valve as the PCUs.

Nair et al. (2018) did not include an explicit PCU-bypass option for a stream. They effected PCU-bypass by allowing a pressure ratio of 1.0 for each PCU. This allowed a stream to enter and reenter the HEN without any pressure change, creating redundant streams. Similarly, they allowed a stream to have zero temperature change in the HEN. This allowed two PCUs to be in a series without any temperature change in between. If we allow a PCU to have multiple stages, then this series arrangement seems undesirable, because two consecutive movers are undesirable. Besides, such a series arrangement needs more stages in the

superstructure to effect a given pressure ratio. To avoid these drawbacks and redundancies, we disallow zero pressure change across any stage except 1, and zero enthalpy change across the HEN of any stage except 1 and the last for each stream s in our superstructure. The bypasses in Figure 4 for stages 2 through K_s help us enforce these requirements. If a stage k is bypassed, then we force all subsequent stages to be bypassed. This eliminates permutations of stages. Zero enthalpy change is allowed across the HEN in the first and the last stage, since these two stages even with zero heat exchanges do not lead to successive PCUs.

4 Optimization Methodology

The superstructure in Figure 4 can be reduced to an optimal HAWEN by solving a complex MINLP as done by previous works (Huang and Karimi, 2016; Nair et al., 2018; and Onishi et al., 2014b). However, as discussed earlier, the MINLP approach has limitations. To overcome them, we propose a simulation-based continuous optimization approach, which does not use any explicit binary variables, but the continuous variables implicitly fix the discrete decisions. This demands a derivative-free optimization algorithm such as particle swarm optimization (PSO) developed by Kennedy and Eberhart (1995). PSO has been successfully applied for rigorous optimization in several studies (Cao et al. 2017; Hamedi et al., 2018; Hamedi et al., 2019; Khan and Lee, 2013; Sadeghzadeh et al., 2015). Some (Clarke et al., 2014; Elbeltagia et al., 2005; Hassan et al. 2005) have shown that it can be computationally more efficient than other metaheuristic methods. For this work, we implemented a PSO algorithm in Matlab and used Aspen HYSYS V9 for simulating networks and estimating thermodynamic properties.

To describe the PSO algorithm, we first define the following notation:

$z(s)$ = Composition of stream s

$F(s)$ = Flow rate of stream s

$HI(s, 1 \leq k \leq K_s)$ = Heat content of stream s, as it exits the HEN in stage k

$HI(s, K_s) = HOUT_s$

$f(s, 1 \leq k \leq K_s)$ = Vapor fraction of stream s, as it exits the HEN in stage k

$H(s, 2 \leq k \leq K_s)$ = Heat content of stream s, as it exits PCS_{sk}; $H(s, 1) = HIN_s$

$P(s, 2 \leq k \leq K_s)$ = Pressure of stream s, as it exits PCS_{sk};

$P(s, 1) = PIN_s$ and $P(s, K_s) = POUT_s$

$W(s, 2 \leq k \leq K_s)$ = Total net power generated (< 0) or consumed (> 0) in PCS_{sk}

The PSO algorithm requires that we define a set of continuous optimization variables that uniquely fix the objective function value. To this end, we define $P(s, 2 \leq k \leq K_s - 1)$ and $HI(s, 1 \leq k \leq K_s - 1)$ as the $2K_s - 3$ optimization variables for each s. When specific numerical values are assigned to these optimization variables, we get what is known as a particle in the context of PSO. Then, for each particle during our PSO algorithm, we do the following to evaluate an objective function (defined later) value for that particle.

1. Set $s = 1$, $k = 2$, and $K_{Last} = K_s$.
2. Compute the pressure ratio across PCS_{sk} as $PR(s, k) = \max[P(s, k), P(s, k-1)] / \min[P(s, k), P(s, k-1)]$.
3. If $PR(s, k) \leq 1 + \epsilon_P$ (where ϵ_P is a small fraction to judge if PCS_{sk} is trivial, and should be bypassed), then do as follows. If $k < K_{Last}$, then set $P(s, k \; to \; K_s) = POUT_s$, $HI(s, k \; to \; K_s) = HOUT_s$, $K_{Last} = k$, and go to 2. Else, set $P(s, k-1) = POUT_s$, $HI(s, k-1) = HOUT_s$, $K_{Last} = k - 1$, $k = k - 1$, and go to 2.
4. Compute $f(s, k)$ by simulating stream s in Aspen HYSYS with $z(s)$, $P(s, k-1)$, and $HI(s, k-1)$ as input data.
5. Reduce Figure 5 appropriately as shown in Table 1.

Table 1. PCU selection based on vapor fractions and pressure ratios

Conditions	Required actions to select appropriate PCUs in Figure 5
If $\{f(s,k) = 0 \;\&\; P(s,k) > P(s,k-1)\}$	Deactivate the valve and expander on the liquid substream. Only pump remains.
If $\{f(s,k) = 0 \;\&\; P(s,k) < P(s,k-1)\}$	Deactivate the pump and select either valve or liquid expander from Appendix A.
If $\{f(s,k) = 1 \;\&\; P(s,k) > P(s,k-1)\}$	Deactivate the valve and expander on the gas substream. Only compressor remains.
If $\{f(s,k) = 1 \;\&\; P(s,k) < P(s,k-1)\}$	deactivate the compressor and select either valve or turbine from Appendix A.
If $\{0 < f(s,k) < 1 \;\&P(s,k) > P(s,k-1)\}$	Deactivate the valve and expander on both substreams. Pump remains on the liquid, and compressor on the gas substream.
If $\{0 < f(s,k) < 1 \;\&\; P(s,k) < P(s,k-1)\}$	Deactivate the compressor, pump, and select either valve or expander from Appendix A for both gas and liquid substreams.

6. Simulate PCS_{sk} to compute $H(s,k)$ and $W(s,k)$.
7. If $|H(s,k) - HI(s,k)| < \epsilon_H$ and $k < K_{Last}$, then set $P(s,k\ to\ K_s) = POUT_s$, $HI(s,k\ to\ K_s) = HOUT_s$, $K_{Last} = k$, and go to 2.
8. If $k < K_{Last}$, then set $k = k + 1$ and go to 2. Otherwise if $s < S$, then set $s = s + 1$, $k = 2$, $K_{Last} = K_s$, and go to 2.
9. Simulate the MSHE module in Aspen HYSYS as described in the following section.
10. Evaluate the objective function.

Figure 6 shows the complete procedure for computing the objective function for any given PSO particle.

4.1 The HEN Simulation

Recall that the HEN is simply an MSHE. We use LNG Exchanger in Aspen HYSYS to simulate it. It requires that all the streams entering the LNG exchanger are added to the module, and their flow rates, compositions, entry and exit temperatures, and entry and exit pressures must be specified except for one unknown, which it computes from the overall energy balance. It then constructs the hot and cold composite curves to compute the minimum temperature approach or MTA for the exchanger. In our superstructure, each process stream s enters the MSHE K_s

times, once in each stage. Each utility stream enters only once in stage 1. Thus, we use the script from Appendix B to install one LNG exchanger, $K_1 + K_2 + \cdots + K_S$ distinct process streams, and the required utility streams. For a given PSO particle, some stages and thus streams may not exist. In this case, we assign dummy but identical entry and exit temperatures and pressures for each such stream. In other words, the heat gain or loss by each such stream is zero, and it does not impact the energy balance. During our PSO algorithm, all the conditions for each MSHE stream will be fully defined for each PSO particle. This means that LNG Exchanger has one extra input, and cannot be simulated as such. To allow that extra input, we must add one degree of freedom artificially. An arbitrary PSO particle may not satisfy the MSHE energy balance. The heat lost by the hot streams may not equal the heat gained by the cold streams. There will be either a hot or a cold deficit. For correcting this deficit, we define two energy flows into LNG Exchanger: cold (Q_c) and heat (Q_h). We effect these energy flows by adding two hypothetical streams (say A and B) with unknown flows into LNG Exchanger: one undergoing phase change at a constant low temperature, and the other at a constant high temperature relative to other stream temperatures. Given any PSO particle, if we specify the flow of A, then LNG Exchanger will fix the flow of B, using the energy balance. Then, for setting the flow of A, we do as follows. For each PSO particle, given the flow of A, LNG Exchanger will compute MTA. In many situations, this MTA will violate its allowable lower limit. In this case, we must increase this MTA by moving the two composite curves farther apart. This can be achieved by increasing Q_A until MTA reaches its lower limit. Thus, we use Adjust in Aspen HYSYS to manipulate Q_A to guarantee the required MTA, and let LNG Exchanger fix Q_B. Since both Q_A and Q_B must be zero in the final solution, we add a penalty term into the objective function to force $Q_A + Q_B = 0$ in the optimal solution.

4.2 Objective Function

Our algorithm allows any objective function as long as it can be computed from the HYSYS simulation of an arbitrary PSO particle. It also allows complete freedom in defining objective functions. In this work, we define three objectives.

Minimum total annualized cost (TAC)

$$TAC = \gamma . CAPEX + OPEX \quad (1)$$

where, CAPEX is the total capital expense, OPEX is the annual operating expense, and γ is the annualization factor for CAPEX. CAPEX includes the total cost of each unit that exists in the process represented by each PSO particle. In other words, CAPEX includes (1) the cost of the MSHE, and (2) the cost of each PCS_{sk} that may exist for a given PSO particle. The cost of PCS_{sk} includes (1) the cost of a separator, if it exists [$0 < f(s,k) < 1$], and (2) the costs of all PCUs that are active in PCS_{sk}. See Appendix C for more details.

Minimum Power Use:

$$Power = \sum_{s=1}^{S} \sum_{k=2}^{K_s} W(s,k) \quad (2)$$

Minimum Exergy Loss:

$$Exergy\ Loss = \sum_{s=1}^{S} \sum_{k=2}^{K_s} W(s,k) - \text{sum of exergy losses for all streams} \quad (3)$$

When the initial and target conditions of all streams are fixed, then the second term becomes constant, and the objective function becomes minimum power use.

We now apply our methodology to two literature case studies and compare results with those available in the literature.

5 The Liquefied Energy Chain (LEC)

This case study (Aspelund et al., 2007; Aspelund and Gundersen, 2009a, 2009b; Wechsung et al. 2011, Onishi et al., 2014a, Nair et al., 2018) involves (1) one onshore LNG regasification terminal, (2) one offshore NG liquefaction plant, (3) one onshore air separation plant, and (4) an oxycombustion power plant. The CO_2 captured from the power plant and N_2 produced by

the air separation plant are liquefied in the regasification terminal using the cold energy from the LNG coming from the offshore LNG plant. The two liquids (LCO2 and LIN) are shipped to liquefy NG at the offshore LNG plant. Table 2 gives the stream data for the LNG plant. Free water at ambient temperature (298.1 K) is the only utility available offshore. The goal is to synthesize an LNG plant that needs no power and meets the targets in Table 2. No targets exist for the exit temperatures of LCO_2 and LIN. While not liquefying the natural gas offshore may be a more logical and economical option for this energy chain, we will assume liquefaction as the objective as done by previous works.

Table 2. Stream data for the LEC (Aspelund et al., 2007)

		Supply		Target	
Stream	Flow (kg/s)	Temperature (K)	Pressure (kPa)	Temperature (K)	Pressure (kPa)
NG	8.10	288.1	6000	109.2	101.32
LIN	8.00	96.15	600	None	101.32
LCO_2	18.00	218.6	550	None	15000

We first consider two previously studied scenarios for this LEC process. Scenario 1 assumes a fixed flow (8 kg/s) of LIN as done by Aspelund et al. (2007). Scenario 2 treats the LIN flow as a variable as done by Wechsung et al. (2011). Aspen HYSYS V9 and the SRK equation of state were used for both scenarios as done by Aspelund et al. (2007) and Wechsung et al. (2011). NG composition was taken from Aspelund et al. (2009a). $K_s = 5$ was assumed for all three process streams (NG, LIN, LCO_2). Cooling water is the utility stream in the MSHE at stage 1. The compressor discharge pressure was limited to16000 kPa.

All computations were done on an Intel® Core (TM) i5-6600 CPU with 3.3 GHz CPU and 16 GB RAM. $c_1 = c_2 = 1.0$ and $0.5 \leq$ (inertia coefficient α) ≤ 1.0 were used as the parameters in the PSO algorithm (Kennedy et al., 2001). The algorithm was limited to 150 iterations, and 15 particles were used for each variable. The PSO algorithm was run 10 times for each scenario to capture the global optimum. Each run took 12-13 hours of real time.

5.1 Scenario I

This scenario corresponds to Case F in Aspelund et al. (2007) with the following assumptions: isentropic efficiency is 85% for all expanders and pumps; polytropic efficiency is 82% for all compressors; MTA $\geq$ 2 K for $T \leq 193\ K$; MTA $\geq$ 3 K for $193.1\ K \leq T \leq 273.1\ K$, and MTA $\geq$ 5 K for $T > 273.1\ K$.

Aspelund et al. (2007) employed their ExPAnD heuristics to obtain the LEC process in Figure 7 for the objective of minimum power use. For a fair comparison, their process was fully simulated except for the pressure drop in the MSHE, which was assumed zero in this study versus 20 kPa in theirs. For a pressure drop of 20 kPa, they reported zero net power production, while our simulation with a pressure drop of zero gives a net power production of 71 kW as shown in Figure 7. Since LNG Exchanger in Aspen HYSYS does not allow multiple temperature-dependent MTAs, MTA was increased gradually from 2 K to 5 K to ensure the multiple MTA limits (MTA $\geq$ 2 K for $T \leq 193\ K$; MTA $\geq$ 3 K for $193.1\ K \leq T \leq 273.1\ K$, and MTA $\geq$ 5 K for $T > 273.1\ K$). After a few runs of our PSO algorithm, MTA = 2.7 K was identified as the one that satisfies all three MTA limits.

Figure 8 shows the process from our algorithm. As in Aspelund et al. (2007), our process also needs no water as utility. However, compared to their process in Figure 7, our process produces 615 kW versus 71 kW of power, does not need any nitrogen compression, and uses only one (versus two) pump for CO_2 before the MSHE. The LIN compressor with a power consumption of 528 kW in Figure 7 is replaced by an expander in our process. The closer tightness of the composite curves in Figure 8 indicates lower exergy losses in our design. A simple exergy calculation (Hinderink et al. 1996) suggests that the exergy loss in the MSHE is reduced by 29% from 586 kW to 416 kW. MSHEs typically destroy a major portion of the input exergy in sub-ambient processes. For this process, the MSHE accounts for about 35% of the entire exergy loss.

If we were to use an MTA limit of 2 K instead of 2.7 K as done above, then our model would yield a higher net power production.

5.2 Scenario 2

This case study corresponds to Case IIId in Wechsung et al. (2011). The objective is to minimize LIN flow, while allowing no thermal utility and zero net power consumption. Wechsung et al. (2011) changed the stream and equipment data (Table 3) from Aspelund et al. (2007). Liquid expanders are not allowed in their study and the liquid expander in Figure 7 is replaced with a valve. The MTA limit was 4 K. Moreover, they made some new assumptions as follows:

a) The isentropic efficiency for LIN compression and expansion is 100% for pressures below 4 MPa and 70% for higher pressures.

b) The compression and expansion of LIN follow the ideal gas model for pressures below 4 MPa.

c) The isentropic efficiency for NG and LCO_2 expansions and compressions is 70%.

d) The efficiency for pumps is 80%.

e) The power for the compression and expansion of LIN was computed using Eq. 1 in their paper, while Aspen HYSYS was used for NG and LCO_2.

f) Each stream is split into several zones with constant heat capacities.

Table 3. Stream data for LEC in Wechsung et al. (2011)

	Supply			Target	
Stream	Flow (kg/s)	Temperature (K)	Pressure (kPa)	Temperature (K)	Pressure (kPa)
NG	1	288.1	7000.0	109.2	101.32
LIN	--	218.6	600.00	---	101.32
LCO_2	2.46	96.15	550.00	---	15000

Figure 9 shows composite curves for the process obtained by Wechsung et al. (2011). Again, for the sake of fair comparison, we simulated it fully with all the above assumptions except assumption (f). To ascertain the impact of this assumption, their composite curves (Figure 9) were reproduced in Aspen HYSYS based on the inlet and outlet temperatures of each stream

split given by Wechsung et al. (2011). For this exercise, the LCO_2 outlet temperature was left free to be fixed by LNG Exchanger. As Figure 9 shows the MSHE has a large temperature cross. This means that the constant heat capacity zones have led to an infeasible MSHE and hence an infeasible process. With such close temperature approaches, the result is not surprising. Figure 10 displays our proposed design for a minimum LIN flow of 0.917 kg/s per kg of LNG versus 0.898 kg reported by Wechsung et al. (2011). It needs three expanders for LIN, one compressor for NG, and produces a net power of 3 kW. More importantly, our process has a very different structure than that of Wechsung et al. (2011).

In order to find an accurate minimum LIN flow for realistic thermophysical properties, this case study was repeated without the assumptions mentioned above. The expansion and compression efficiencies were set as in Scenario I. The MTA limit was 4 K. However, liquid expanders were not allowed. Figure 11 shows the process scheme with a minimum LIN flow of 0.979 kg/s. As it is expected, this is higher than 0.917 kg/s, which was attained with the assumption of ideal gas. In contrast to Wechsung et al. (2011), our process avoids the recompression of nitrogen. It also does not need any external power.

While Onishi et al. (2014a) and Nair et al. (2018) also studied the LEC process, their scope was very limited, and they minimized TAC, so we did not compare our results with them. However, we now consider a more challenging scenario of the LEC process.

5.3 Scenario 3

In all the previous work on this process, LIN was the only stream whose pressure was allowed to change. We now show that this may not be the best strategy. We take all the data, parameters, and objective from scenario 1 except for the LIN flow, which is reduced by 17% to 6.6 kg/s. MTA is set to 2 K irrespective of the temperature zone. Liquid expansion is not allowed.

Figure 12 shows the best process from our algorithm along with the MSHE composite curves. It produces 1272 kW of power, and does not use water. Interestingly, NG rather than

LIN forms an open refrigeration cycle. NG is compressed to 16 MPa (the highest allowed discharge pressure), cooled, and throttled in a valve to provide refrigeration. In contrast, LIN is pumped to 6390 kPa (above its critical pressure), and expanded three times to cool NG after each step. The choice of NG instead of LIN seems logical, because nitrogen has a much higher heat capacity ratio than LNG, hence its compression is more power-intensive. In fact, nitrogen compression is avoided as long as the NG flow and its lowest allowable temperature (ambient for this problem) are adequate to meet the cooling demand.

6 Conclusion

Integrating work and heat are crucial for sub-ambient processes, since they are typically energy intensive and need more complicated networks compared to above-ambient processes. An optimal network can lead to significant energy and cost savings. In this paper, a comprehensive classification of work-heat integration problems was presented, and the adverse impact of using approximate physical properties was highlighted through literature examples. A modified superstructure was then proposed to eliminate trivial solutions and redundant combinatorial scenarios from previous superstructures in the literature. Furthermore, a novel simulation-based metaheuristic optimization methodology was also proposed for the first time to solve WHEN problems. The proposed methodology is more accurate and simpler than the previous works, as it does not need any simplifying assumptions and does not solve complex MINLPs. This algorithm could produce superior results compared to previous approaches, as illustrated by three scenarios of a literature case study on a liquefied energy chain.

7 Acknowledgements

Homa Hamedimastanabad acknowledges the financial support under the SINGA scholarship. The work was also funded in part by the National University of Singapore through a seed grant (R261-508-001-646/733) for a Center of Excellence for Natural Gas.

8 Nomenclature

Abbreviations

CAPEX	Capital Expenses
CPI	Chemical Process Industry
ExPAnD	Extended Pinch Analysis and Design
HE	Heat Exchange
HEN	Heat Exchange Network
HENS	Heat Exchange Network Synthesis
HAWEN	Heat And Work Exchange Network
LCO2	Liquid CO_2
LEC	Liquefied Energy Chain
LIN	Liquid Inert Nitrogen
LNG	Liquefied Natural Gas
MINLP	Mixed Integer Nonlinear Programming
MSHE	Multi Stream Heat Exchanger
MTA	Minimum Temperature Approach
NG	Natural Gas
OPEX	Operating Expenses
PCU	Pressure Changing Unit
PCS	Pressure Changing Stage
PFD	Process Flow Diagram
PSO	Particle Swarm Optimization
SRK	Soave Redlich Kwong
TAC	Total Annualized Cost
WHEN	Work-integrated Heat Exchange Network

WHENS	Work-integrated Heat Exchange Network Synthesis
WE	Work Exchange
WEN	Work Exchange Network
WENS	Work Exchange Network Synthesis
WED	Work Exchange Device

Superstructure Variables, Parameters and Subscripts

f	Vapor Fraction
F	Flowrate
H	Enthalpy after PCUs
HI	Enthalpy after HENs
HIN	Inlet (supply) Enthalpy
$HOUT$	Outlet (target) Enthalpy
k	WHEN Stage Counter
K_s	WHEN Stage Number for Stream s
K_{Last}	Last Stage Number
P	Pressure
PIN	Inlet (supply) Pressure
$POUT$	Outlet (target) Pressure
W	Work Produced or Consumed by PCUs
PR	Pressure Ratio
Q	Hot/Cold Utility Duty
s	Stream Counter
S	Number of Streams
z	stream compositions
γ	Annualization factor

9 Appendix A

Valves and gas/liquid expanders can be used for a process stream with a depressurization need. Valves with a negligible capital cost lead to a large exergy destruction. In contrast, gas/liquid expanders with high capital costs utilize the exergy to generate power. Therefore, there is a trade-off between them. If the objective function is exergy consumption minimization, valves on both liquid and gas substreams should be deactivated. However, if the objective function is TAC, a lower limit for the gas/liquid expander power generation should be identified, below which the equipment is not economical and should be replaced by a valve. Thus, the break-even power of a gas/liquid expander is defined by the following equations. These are the points where the annual power generation revenue of the expander and its annualized capital cost are equal.

$$BEPP_{LE} = \frac{\gamma \times C_{lE}(Pin,Pout,Flowrate)}{MTEPCE \times EP} \quad \text{Eq. A.1}$$

Similarly, $BEPP_{GE}$ is defined:

$$BEPP_{GE} = \frac{\gamma \times C_{GE}(Pin,Pout,Flowrate)}{MTEPCE \times EP} \quad \text{Eq. A.2}$$

where $BEPP_{LE}$ and C_{LE} are the break-even-point for power and capital cost of a liquid expander. $BEPP_{GE}$ and C_{GE} are the break-even-point for power and capital cost of a gas expander. γ, EP and $MTEPCE$ denote the annualizing factor, the electricity selling price per unit and mechanical to electrical power conversion efficiency. When the objective function is exergy consumption minimization, both $BEPP_{GE}$ and $BEPP_{LE}$ should considered zero.

10 Appendix B

a) MSHE Creation Script: The following script creates an MSHE in Aspen HYSYS without any streams attached to it.

```
Specify "FlowSht.1" ":Selection.400"  "ObjectType:LngOpObject"
Message "FlowSht.1" "CreateFromPFD LngOpObject"
SpecWhileSolving Message "FlowSht.1" "DoAutoConnect"
Message "FlowSht.1/UnitOpObject.400(LNG-100)" "IncrementWPFForm"
```

Specify "FlowSht.1/UnitOpObject.400(LNG-100)" ":Enum.590" 0.000000000000e+000

Specify "FlowSht.1/UnitOpObject.400(LNG-100)" ":Enum.590" 0.000000000000e+000

Message "FlowSht.1/UnitOpObject.400(LNG-100)" "DeleteSide 0 0"

Message "FlowSht.1/UnitOpObject.400(LNG-100)" "DeleteSide 0 0"

b) MSHE Stream Creation: The following script creates streams connected to the MSHE as many as it is invoked from the Matlab code. This script is an example for streams 1-2 and 1-2i. Stream 1-2 denotes Stream 1 entering the MSHE for the second time or the second stage. Stream 1-2i denotes the corresponding outlet stream. If there are N streams involved in the MSHE, the following script should be invoked from Matlab N times while changing the stream name according to the stream and stage counters.

Message "FlowSht.1/UnitOpObject.400(LNG-100)" "IncrementWPFForm"

Message "FlowSht.1/UnitOpObject.400(LNG-100)" "AddSide"

AttachObject "FlowSht.1/UnitOpObject.400(LNG-100)" ":MaterialStream.400.14" "NullObject" Create "1-2"

AttachObject "FlowSht.1/UnitOpObject.400(LNG-100)" ":MaterialStream.401.14" "NullObject" Create "1-2i"

Specify "FlowSht.1/UnitOpObject.400(LNG-100)/ExchSide.500.14" ":PressureDrop.300" 0.000000000000e+000

11 Appendix C

$$Minimize\ TAC = \gamma . CAPEX + OPEX \quad \text{Eq. C.1}$$

where γ, CAPEX, OPEX are the annualizing factor, capital expenditure and operating expenses, respectively.

$$CAPEX = C_{MSHE} + \sum_{s=1}^{S} \sum_{k=2}^{k_s} C_{PCU}^{Active}(s,k) \quad \text{Eq. C.2}$$

$$C_{MSHE} = V_{MSHE} \times VPC(V_{MSHE}) \quad \text{Eq. C.3}$$

$C_{PCU}^{Active}(s,k)$ is the cost of active $PCU\ (s,k)$ including required motors or generators. It can be calculated based on the PCU inlet and outlet conditions, and its polytropic/isentropic efficiency. C_{MSHE} is MSHE cost based on the required volume of heat exchanger (V_{MSHE}). V_{MSHE} is a function of the product of overall heat transfer area (A) and overall heat transfer coefficient (U). VPC is a volumetric price curve of the MSHE.

$$OPEX = EC \times \sum_{s=1}^{S} \sum_{\substack{k=2 \\ W(s,k)>0}}^{k_s} W(s,k)/ETMPCE + EP \times \sum_{s=1}^{S} \sum_{\substack{k=2 \\ W(s,k)<0}}^{k_s} W(s,k) \times MTEPCE + \sum_{s \in Utilities} C(s) \times F(s) \quad \text{Eq. C.4}$$

where EC and EP are the electricity cost and the electricity selling price per unit. $ETMPCE$ and $MTEPCE$ denote electrical to mechanical power conversion efficiency and mechanical to electrical power conversion efficiency, respectively. C denotes the cost of utility streams.

12 References

Amini-Rankouhi, A., Huang, Y. (2017). Prediction of maximum recoverable mechanical energy via work integration: A thermodynamic modeling and analysis approach. AIChE Journal, 63(11), 4814-4826. doi:10.1002/aic.15813

Aspelund, A., Berstad, D.O., Gundersen, T. (2007). An Extended Pinch Analysis and Design procedure utilizing pressure based exergy for subambient cooling. Applied Thermal Engineering, 27(16 SPEC. ISS.), 2633-2649. doi:10.1016/j.applthermaleng.2007.04.017

Aspelund, A., Gundersen, T. (2009a). A liquefied energy chain for transport and utilization of natural gas for power production with CO2 capture and storage - Part 1. Applied Energy, 86(6), 781-792. doi:10.1016/j.apenergy.2008.10.010

Aspelund, A., Gundersen, T. (2009b). A liquefied energy chain for transport and utilization of natural gas for power production with CO2 capture and storage - Part 2: The offshore and the onshore processes. Applied Energy, 86(6), 793-804. doi:10.1016/j.apenergy.2008.10.022

Li, B.H., Castillo, Y. E. C., Chang, C.T. (2019). An improved design method for retrofitting industrial heat exchanger networks based on Pinch Analysis. Chemical Engineering Research and Design, 148, 260-270. doi:10.1016/j.cherd.2019.06.008

Cao, Y., Flores-Cerrillo, J., Swartz, C. L. E. (2017). Practical optimization for cost reduction of a liquefier in an industrial air separation plant. Computers and Chemical Engineering, 99, 13-20. doi:10.1016/j.compchemeng.2016.12.011

Clarke, J., McLay, L., McLeskey Jr, J. T. (2014). Comparison of genetic algorithm to particle swarm for constrained simulation-based optimization of a geothermal power plant. Advanced Engineering Informatics, 28(1), 81-90. doi:10.1016/j.aei.2013.12.003

Duran, M. A., Grossmann, I. E. (1986). Simultaneous optimization and heat integration of chemical processes. AIChE Journal, 32(1), 123-138. doi:10.1002/aic.690320114

Elbeltagi, E., Hegazy, T., Grierson, D. (2005). Comparison among five evolutionary-based optimization algorithms. Advanced Engineering Informatics, 19(1), 43-53. doi:10.1016/j.aei.2005.01.004

Fu, C., Gundersen, T. (2015a). Integrating compressors into heat exchanger networks above ambient temperature. AIChE Journal, 61(11), 3770-3785. doi:10.1002/aic.15045

Fu, C., Gundersen, T. (2015b). Integrating expanders into heat exchanger networks above ambient temperature. AIChE Journal, 61(10), 3404-3422. doi:10.1002/aic.14968

Fu, C., Gundersen, T. (2015c). Sub-ambient heat exchanger network design including compressors. Chemical Engineering Science, 137, 631-645. doi:10.1016/j.ces.2015.07.022

Fu, C., Gundersen, T. (2015d). Sub-ambient heat exchanger network design including expanders. Chemical Engineering Science, 138, 712-729. doi:10.1016/j.ces.2015.09.010

Fu, C., Gundersen, T. (2016a). Correct integration of compressors and expanders in above ambient heat exchanger networks. Energy, 116, 1282-1293. doi:10.1016/j.energy.2016.05.092

Fu, C., Gundersen, T. (2016b). Heat and work integration: Fundamental insights and applications to carbon dioxide capture processes. Energy Conversion and Management, 121, 36-48. doi:10.1016/j.enconman.2016.04.108

Grossmann I.E., Yeomans H., Kravanja Z. (1998). A rigorous disjunctive optimization model for simultaneous flowsheet optimization and heat integration. Computers and Chemical Engineering, 22, S157-S164. doi:10.1016/S0098-1354(98)00050-7

Hamedi, H., Karimi, I.A., Gundersen, T. (2018). Optimal cryogenic processes for nitrogen rejection from natural gas. Computers and Chemical Engineering, 112, 101-111. doi:10.1016/j.compchemeng.2018.02.006

Hamedi, H., Karimi, I.A., Gundersen, T. (2019). Optimization of helium extraction processes integrated with nitrogen removal units: A comparative study. Computers and Chemical Engineering, 121, 354-366. doi:10.1016/j.compchemeng.2018.11.002

Hasan, M.M.F., Karimi, I.A., Alfadala, H.E., Grootjans, H. (2009a). Operational modeling of multistream heat exchangers with phase changes. AIChE Journal, 55(1), 150-171. doi:10.1002/aic.11682

Hasan, M.M.F., Jayaraman, G., Karimi, I.A., Alfadala, H.E. (2009b). Synthesis of heat exchanger networks with nonisothermal phase changes. AIChE Journal, 56(4), 930-945. doi:10.1002/aic.12031

Hassan, R., Cohanim, B., De Weck, O., Venter, G. (2005). A comparison of particle swarm optimization and the genetic algorithm. 46th AIAA/ASME/ASCE/AHS/ASC Structures, Structural Dynamics and Materials Conference Austin, Texas. doi:10.2514/6.2005-1897

Hinderink, A.P., Kerkhof, F.P.J.M., Lie, A.B.K., De Swaan Arons, J., Van Der Kooi, H.J., 1996. Exergy analysis with a flowsheeting simulator - I. Theory; calculating exergies of material streams. Chemical Engineering Science, 51(20), 4693-4700. doi: 10.1016/0009-2509(96)00220-5

Huang, K., Karimi, I. A. (2016). Work-heat exchanger network synthesis (WHENS). Energy, 113, 1006-1017. doi:10.1016/j.energy.2016.07.124

Huang, Y. L., Fan, L. T. (1996). Analysis of a Work Exchanger Network. Industrial & Engineering Chemistry Research, 35(10), 3528-3538. doi:10.1021/ie9507383

Kamath, R.S., Biegler, L.T., Grossmann, I.E. (2012). Modeling multistream heat exchangers with and without phase changes for simultaneous optimization and heat integration. AIChE Journal, 58(1), 190-204. doi:10.1002/aic.12565

Kennedy, J., Eberhart, R. (1995). Particle swarm optimization. Proceedings of the 1995 the IEEE International Conference on Neural Networks, Perth, Australia, 4, 1942-1948.

Kennedy, J., Eberhart, R., Shi, Y. (2001). Swarm Intelligence. Morgan Kaufmann.

Khan, M. S., & Lee, M. (2013). Design optimization of single mixed refrigerant natural gas liquefaction process using the particle swarm paradigm with nonlinear constraints. Energy, 49(1), 146-155. doi:10.1016/j.energy.2012.11.028

Liu, G., Zhou, H., Shen, R., Feng, X. (2014). A graphical method for integrating work exchange network. Applied Energy, 114, 588-599. doi:10.1016/j.apenergy.2013.10.023

Nair, S. K., Nagesh Rao, H., Karimi, I. A. (2018). Framework for work-heat exchange network synthesis (WHENS). AIChE Journal, 64(7), 2472-2485. doi:10.1002/aic.16129

Nair, S. K., Karimi, I. A. (2019). Unified Heat Exchanger Network Synthesis via a Stageless Superstructure. Industrial and Engineering Chemistry Research, 58 (15), 5984–6001. doi:10.1021/acs.iecr.8b04490

Onishi, V. C., Ravagnani, M. A. S. S., Caballero, J. A. (2014a). Simultaneous synthesis of heat exchanger networks with pressure recovery: Optimal integration between heat and work. AIChE Journal, 60(3), 893-908. doi:10.1002/aic.14314

Onishi, V. C., Ravagnani, M. A. S. S., Caballero, J. A. (2014b). Simultaneous synthesis of work exchange networks with heat integration. Chemical Engineering Science, 112, 87-107. doi:10.1016/j.ces.2014.03.018

Onishi, V. C., Quirante, N., Ravagnani, M. A. S. S., Caballero, J. A. (2018). Optimal synthesis of work and heat exchangers networks considering unclassified process streams at sub and bove-ambient conditions. Applied Energy, 224, 567-581. doi:10.1016/j.apenergy.2018.05.006

Pavão, L. V.; Costa, C. B. B.; Ravagnani, M. A. S. S. (2019), A new framework for work and heat exchange network synthesis and optimization. Energy Conversion and Management, 183, 617-632. doi:10.1016/j.enconman.2019.01.018

Quirante, N., Grossmann I.E., Caballero, J.A. (2018). Disjunctive model for the simultaneous optimization and heat integration with unclassified streams and area estimation. Computers and Chemical Engineering, 108, 217-231. doi:10.1016/j.compchemeng.2017.09.013

Razib, M.S., Hasan, M.M.F., Karimi, I.A. (2012). Preliminary synthesis of work exchange networks. Computers and Chemical Engineering, 37, 262-277. doi:10.1016/j.compchemeng.2011.09.007

Sadeghzadeh, H., Ehyaei, M. A., Rosen, M. A. (2015). Techno-economic optimization of a shell and tube heat exchanger by genetic and particle swarm algorithms. Energy Conversion and Management, 93, 84-91. doi:10.1016/j.enconman.2015.01.007

Watson, H.A.J., Khan, K.A., Barton, P.I. (2015). Multistream heat exchanger modeling and design. AIChE Journal, 61(10), 3390-3403. doi:10.1002/aic.14965

Wechsung, A., Aspelund, A., Gundersen, T., Barton, P. I. (2011). Synthesis of heat exchanger networks at subambient conditions with compression and expansion of process streams. AIChE Journal, 57(8), 2090-2108. doi:10.1002/aic.12412

Yang, A., Jin, S., Shen, W., Cui, P., Chien, I. L., Ren, J. (2019). Investigation of energy-saving azeotropic dividing wall column to achieve cleaner production via heat exchanger network and

heat pump technique. Journal of Cleaner Production, 234, 410-422. doi: 10.1016/j.jclepro.2019.06.224

Yee, T.F., Grossmann, I.E., Kravanja, Z. (1990). Simultaneous optimization models for heat integration—I. Area and energy targeting and modeling of multi-stream exchangers. Computers and Chemical Engineering, 14 (10), 1151-1164. doi:10.1016/0098-1354(90)85009-Y

Yee, T.F., Grossmann, I.E. (1990). Simultaneous optimization models for heat integration II. Heat exchanger network synthesis. Computers and Chemical Engineering, 14 (10), 1165–1184. doi:10.1016/0098-1354(90)85010-8

Yu, H.; Fu, C.; Vikse, M.; He, C.; Gundersen, T.(2019). Identifying optimal thermodynamic paths in work and heat exchange network synthesis. AIChE Journal, 65 (2), 549-561. doi: 10.1002/aic.16437

Zhuang, Y., Liu, L., Zhang, L.; Du, J., Shen, S. (2019). An extended superstructure modeling method for simultaneous synthesis of direct work exchanger networks. Chemical Engineering Research and Design, 144, 258-27. doi:10.1016/j.cherd.2019.02.022

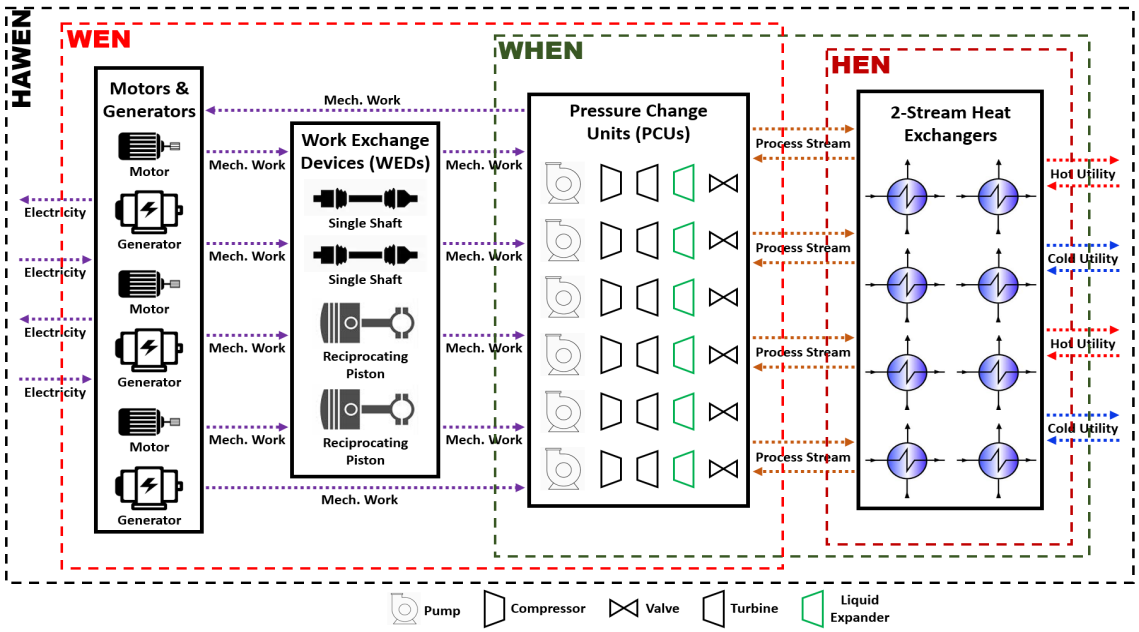

Figure 1. Classification and scopes of various energy integration problems.

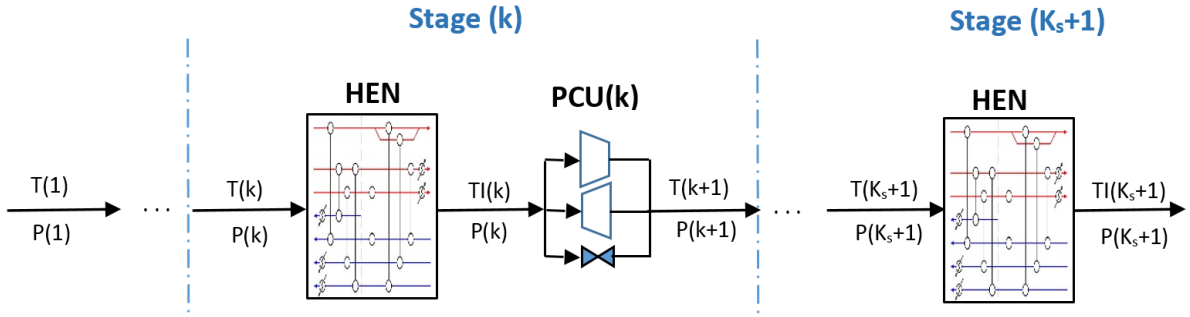

Figure 2. The superstructure for stream *s* in the HAWENS model of Nair et al. (2018)

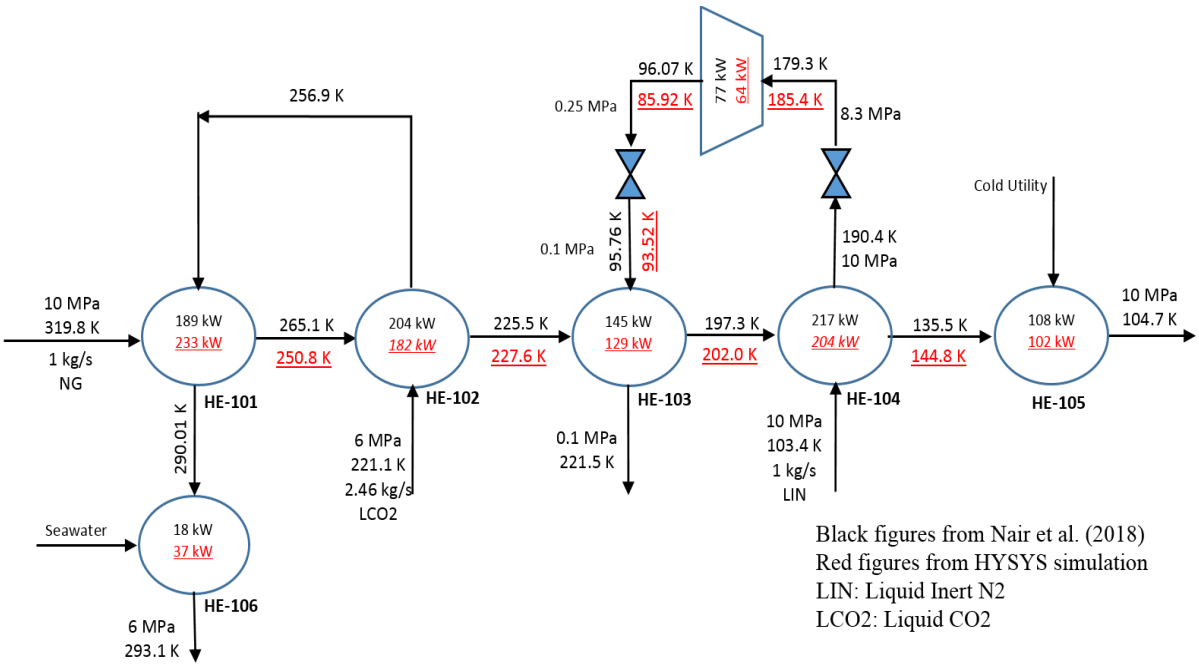

Figure 3. Discrepancies between the correlation-based results of Nair et al. (2018) and those from Aspen HYSYS simulation.

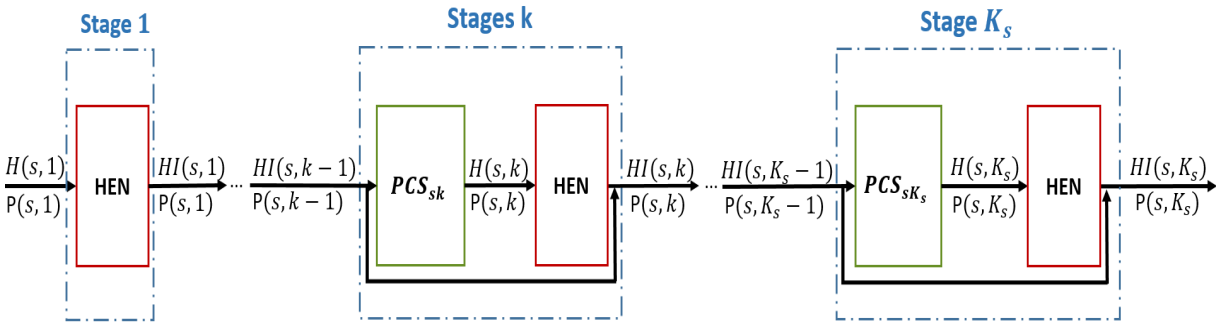

Figure 4. The superstructure for stream s

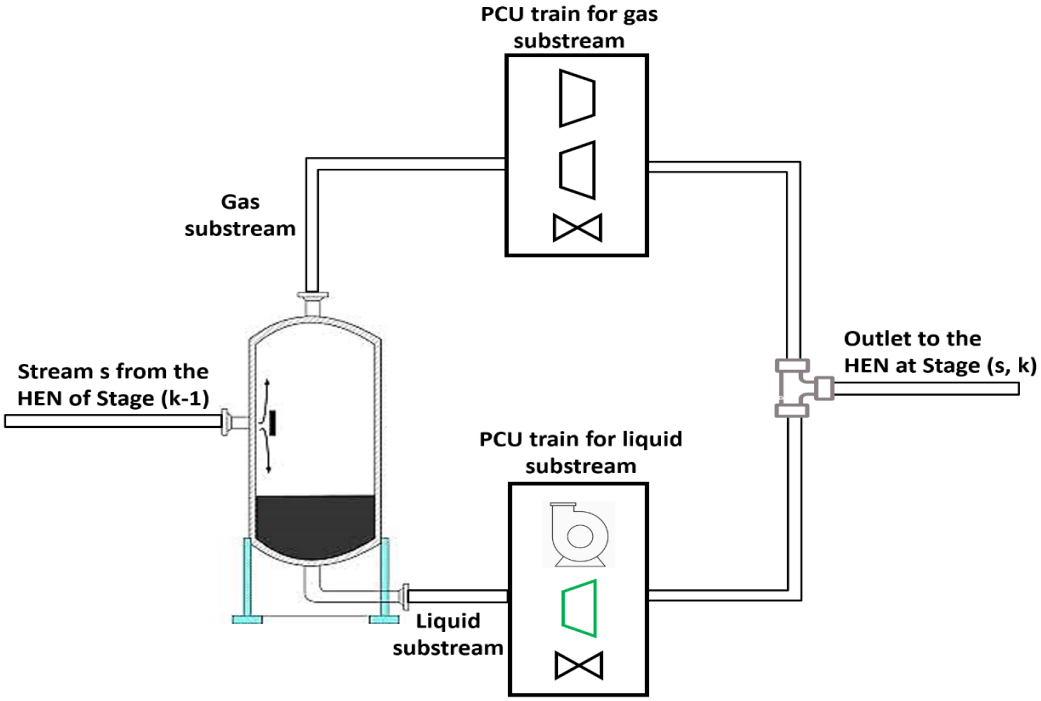

Figure 5. PCS for stage k of stream s

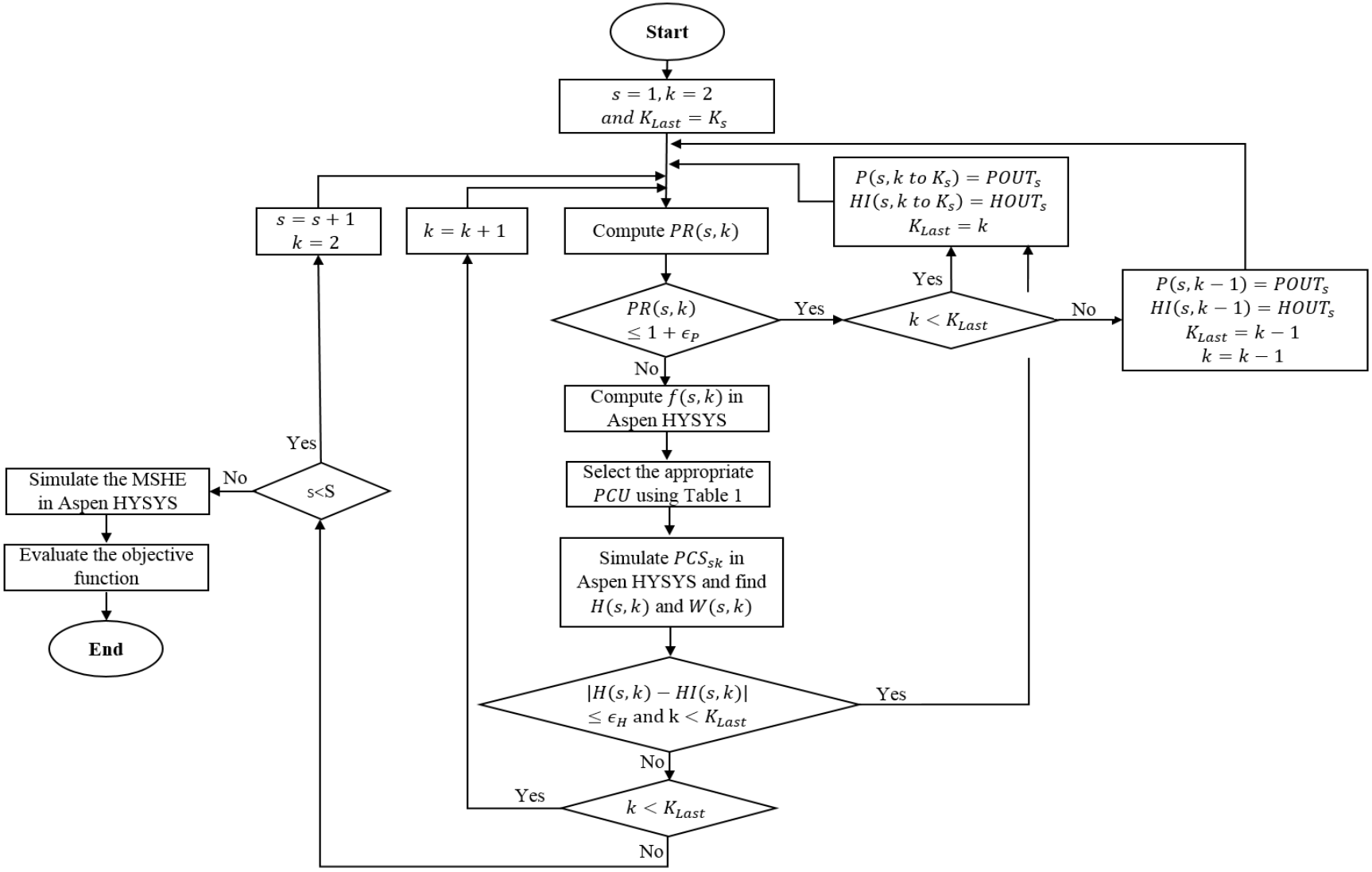

Figure 6. Objective function evaluation flowchart for a PSO particle

a)

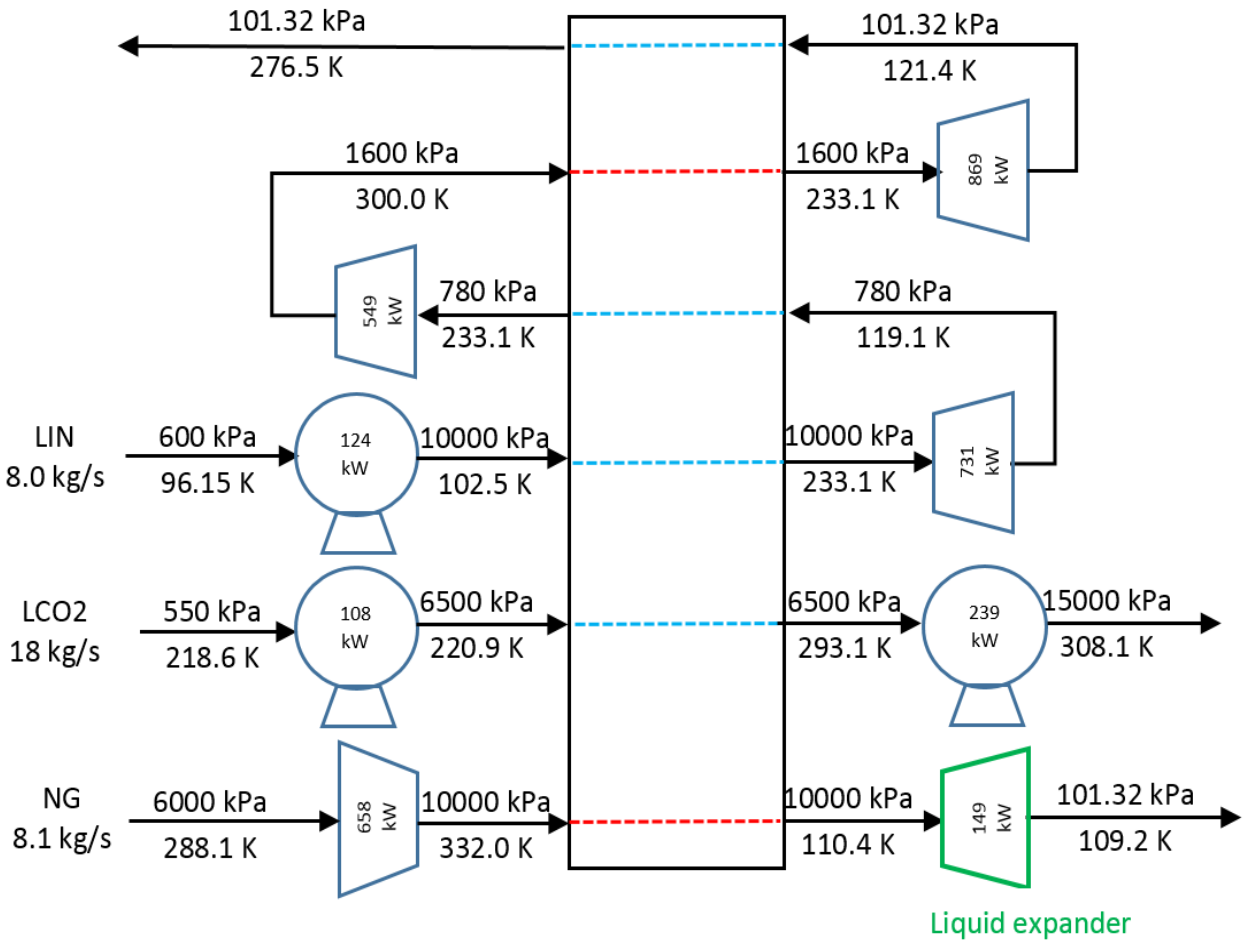

b)

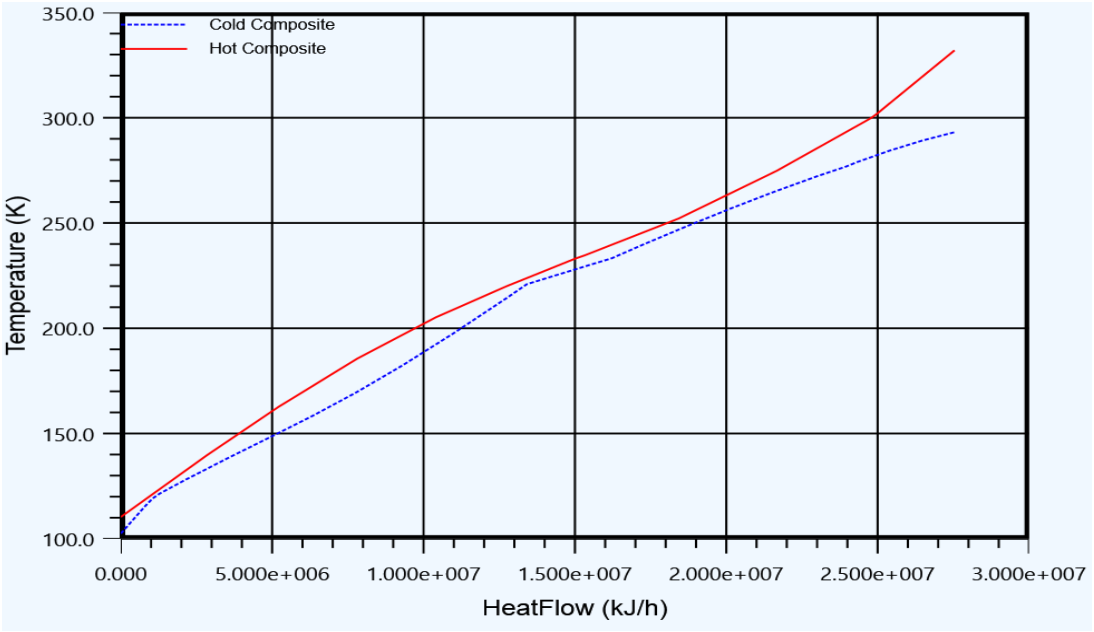

Figure 7. a) PFD b) CCs for the LEC offshore section proposed by Aspelund et al. (2007)

a)

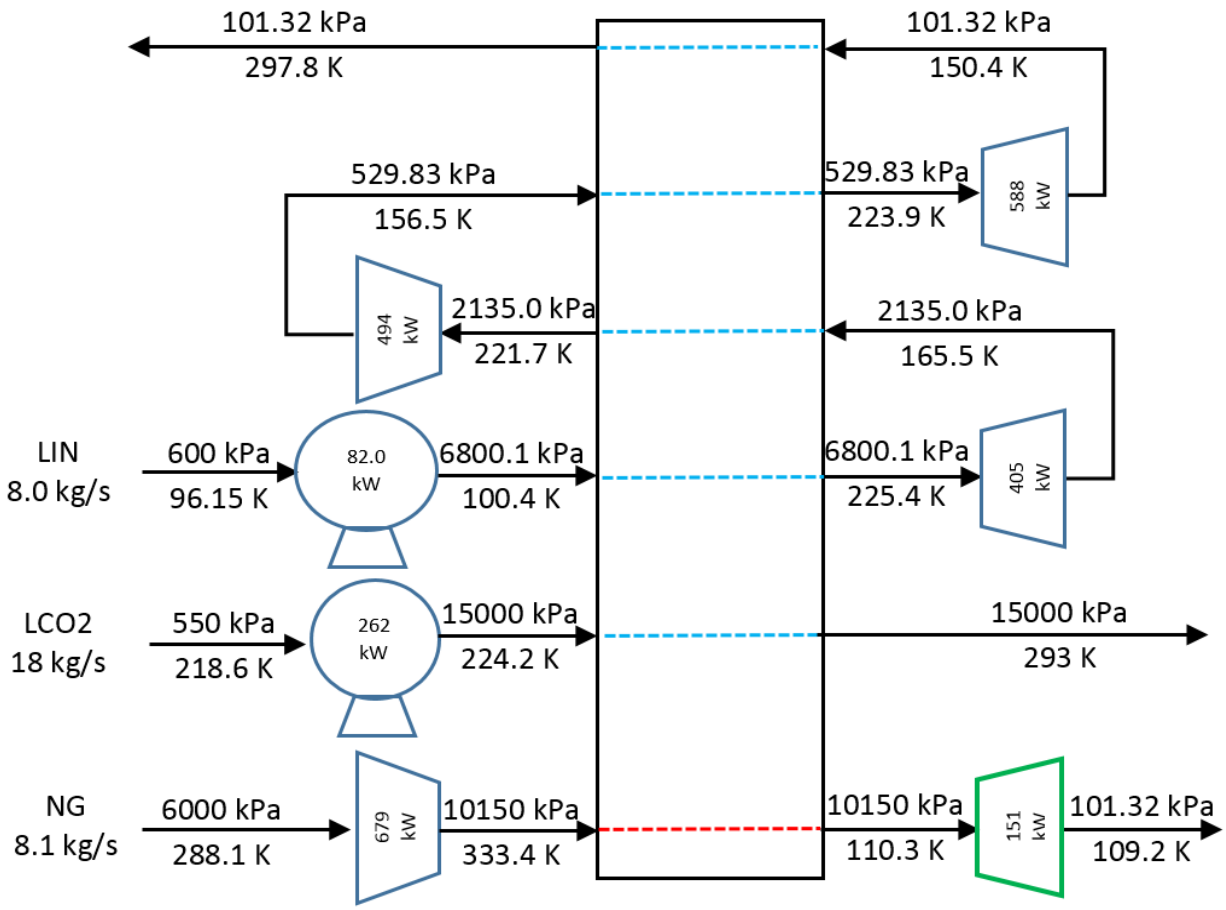

b)

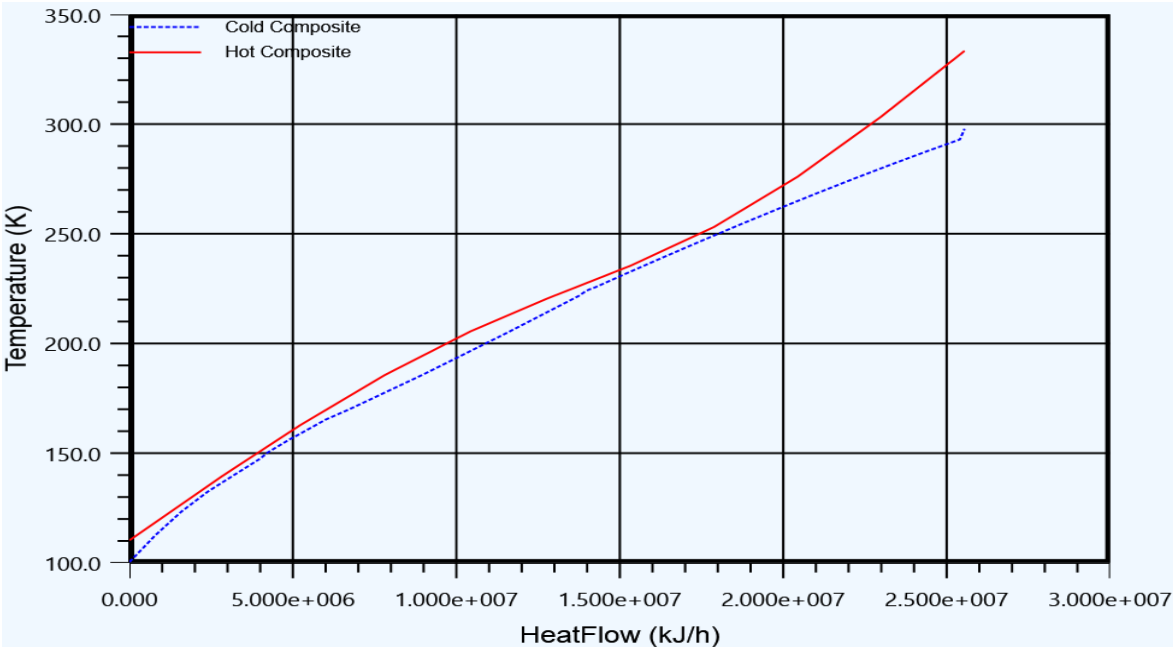

Figure 8. The optimal a) PFD b) CCs for Scenario I developed by our superstructure

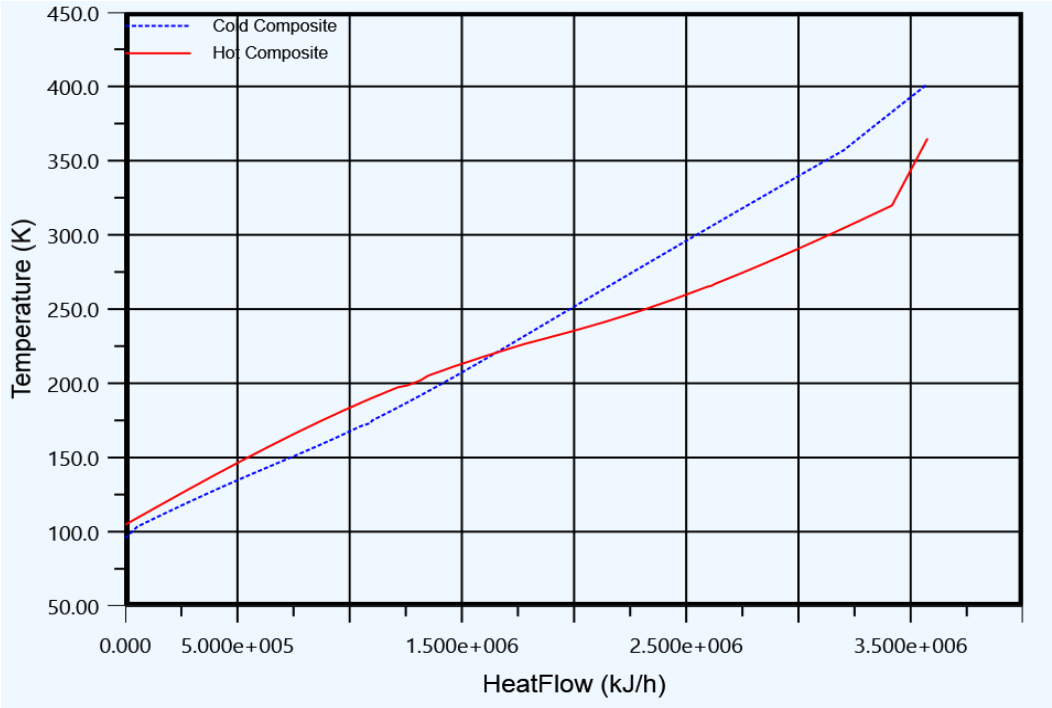

Figure 9. CCs for Scenario II developed by Wechsung et al. (2011)

a)

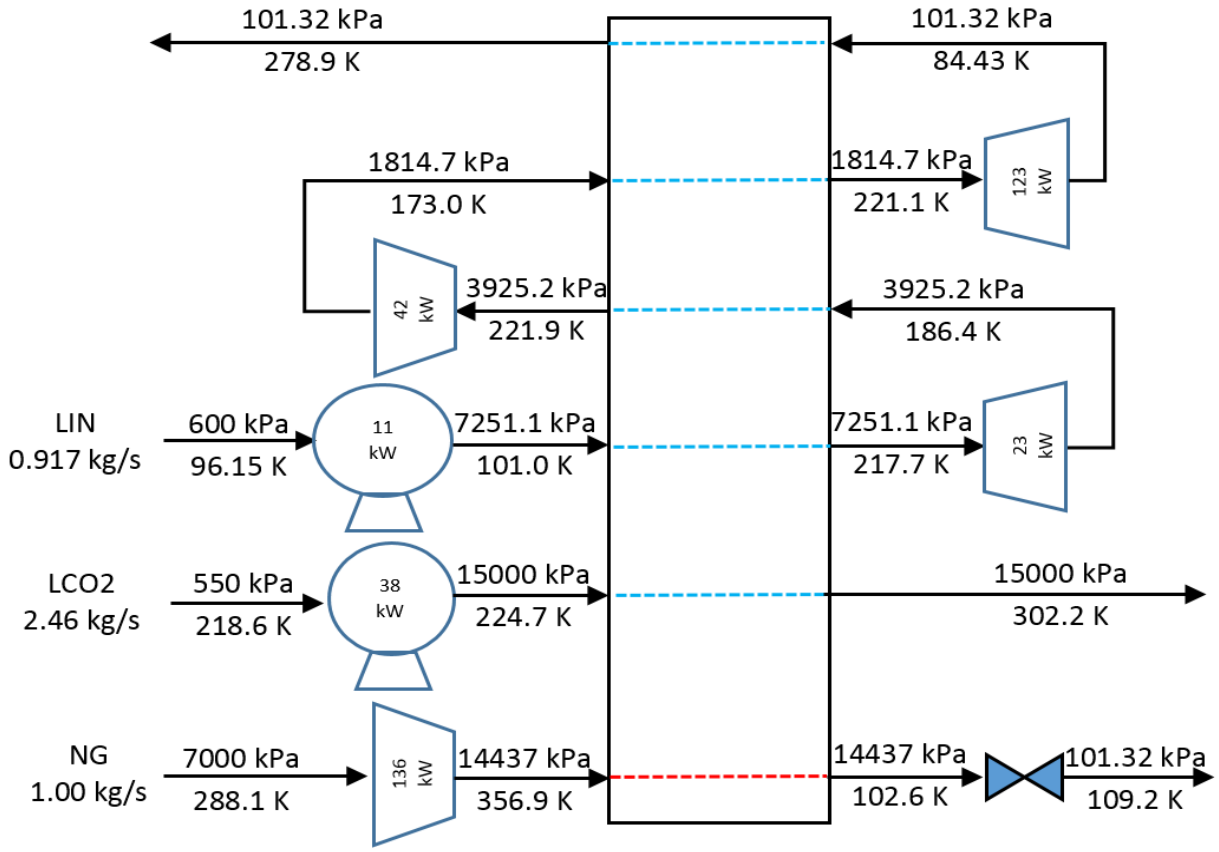

b)

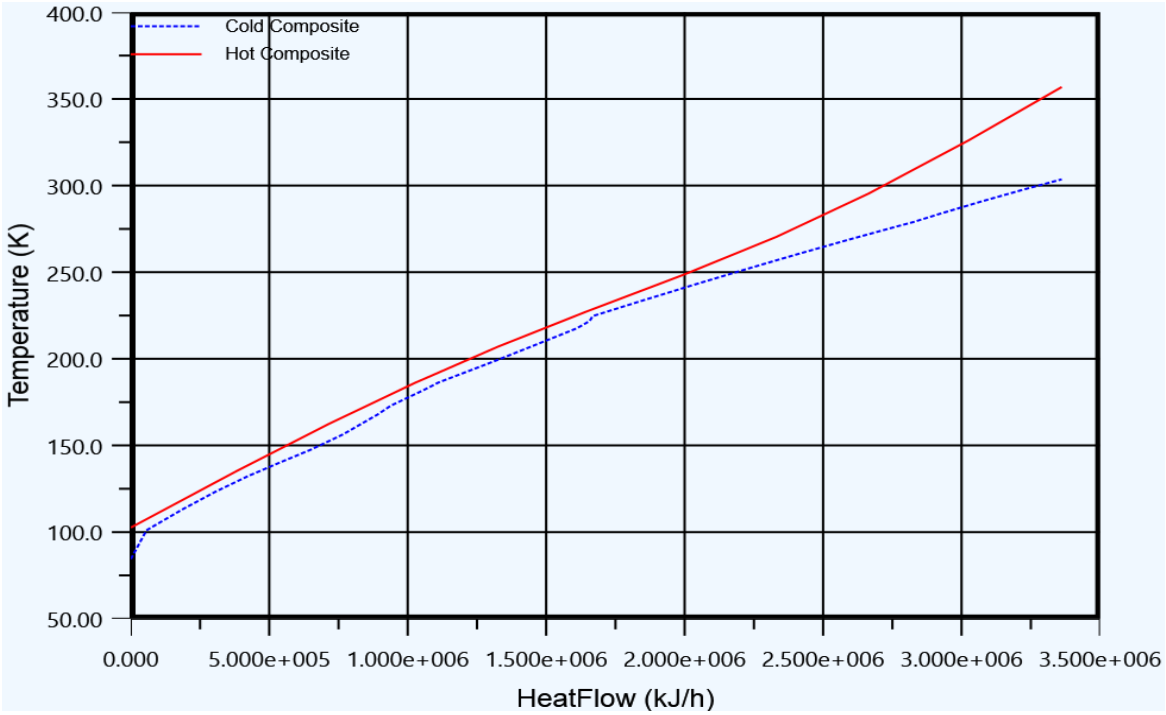

Figure 10. The optimal a) PFD b) CCs for Scenario II with 5 assumptions from Wechsung et al. (2011)

a)

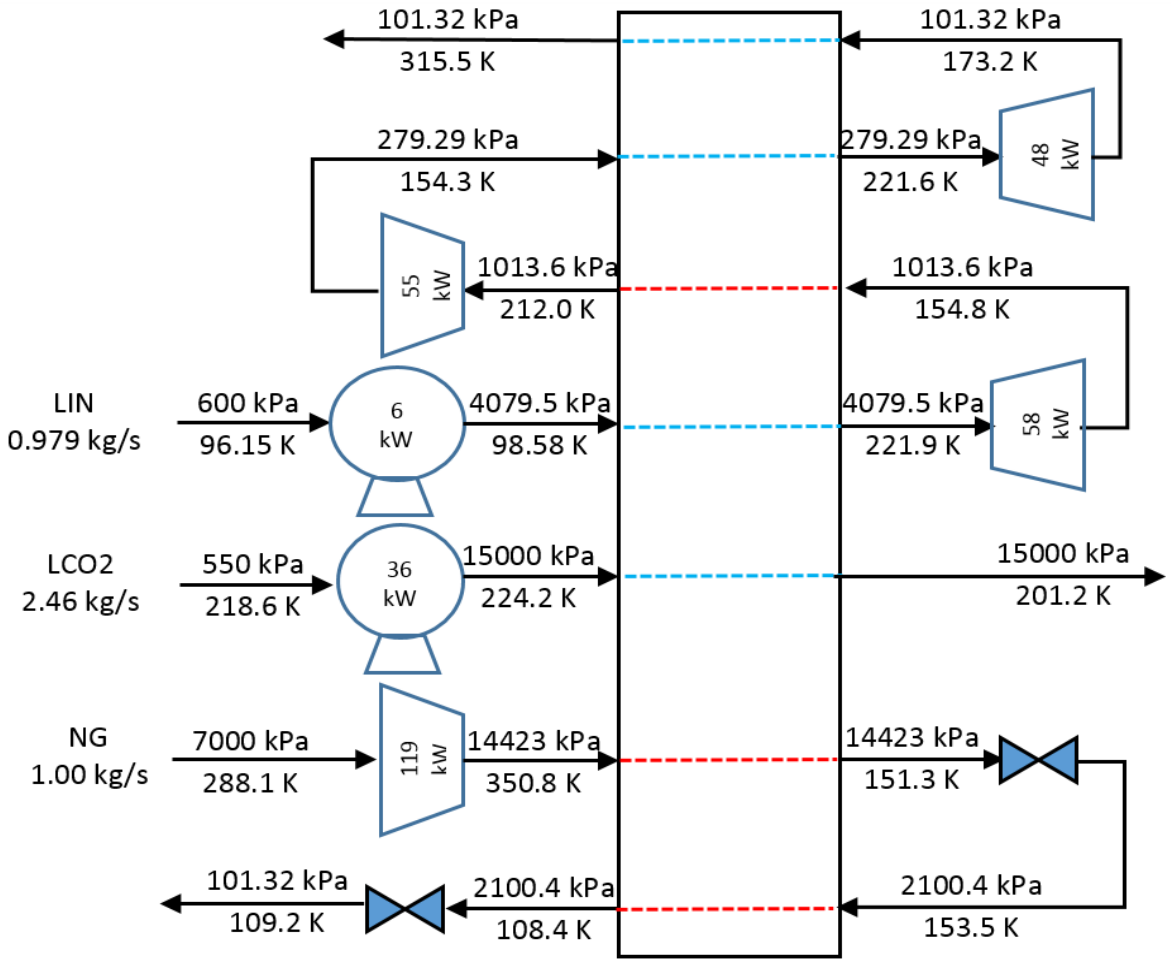

b)

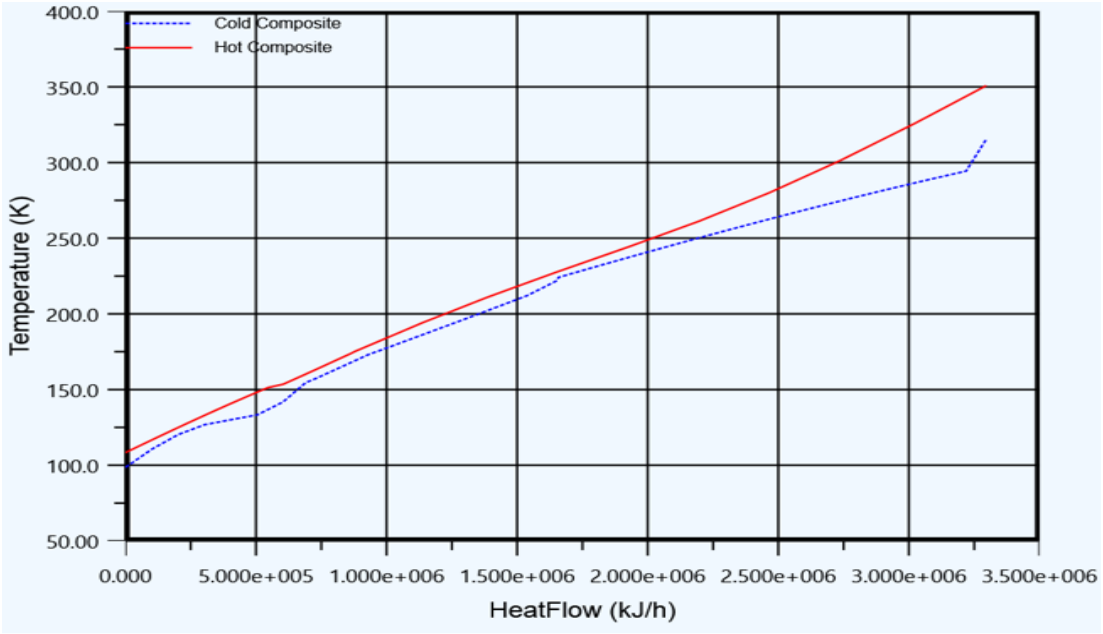

Figure 11. The optimal a) PFD b) CCs for Scenario II without any assumptions

a)

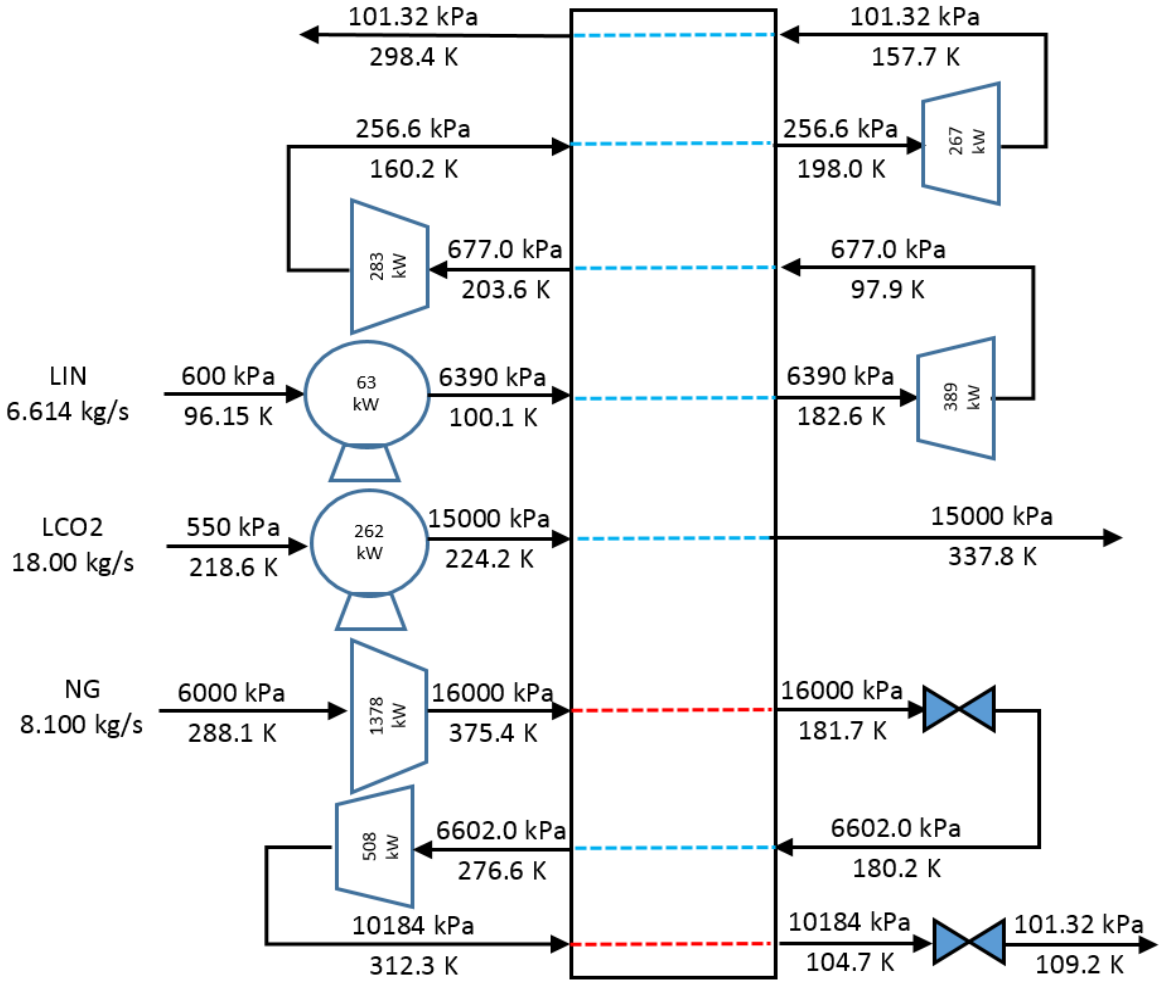

b)

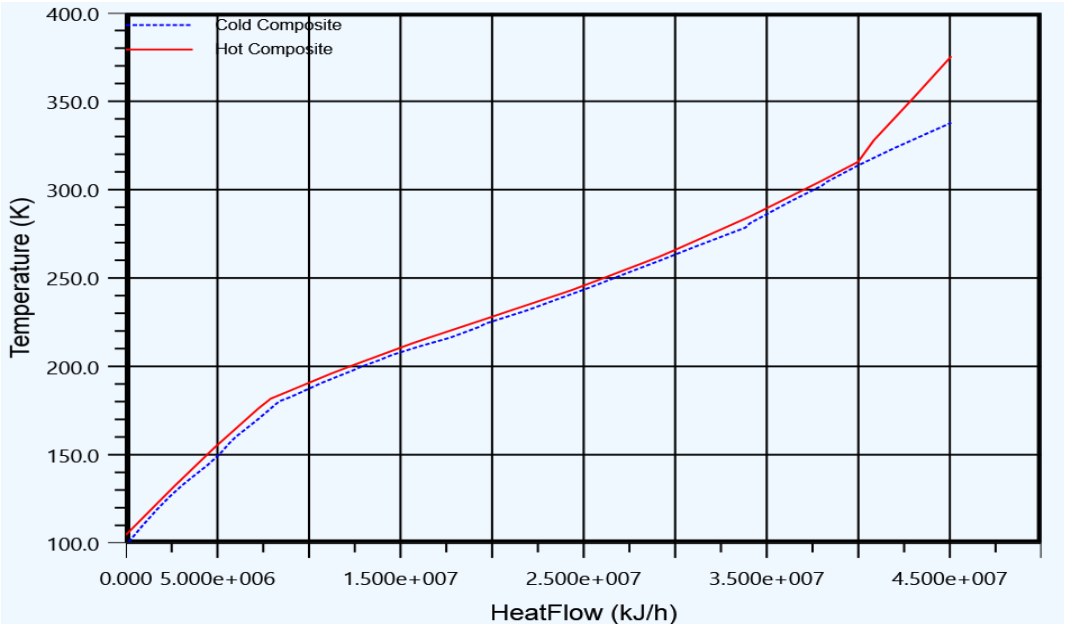

Figure 12. The optimal a) PFD b) CCs for Scenario III developed by our superstructure